Radiosensitization by irinotecan is attributed to G2/M phase arrest, followed by enhanced apoptosis, probably through the ATM/Chk/Cdc25C/Cdc2 pathway in p53-mutant colorectal cancer cells

YAQI WANG[1,2*], LIFENG YANG[1,2*], JING ZHANG[1,2*], MENGLONG ZHOU[1,2], LIJUN SHEN[1,2], WEIJUAN DENG[1,2], LIPING LIANG[1,2], RAN HU[1,2], WANG YANG[1,2], YE YAO[1,2], HUI ZHANG[1,2] and ZHEN ZHANG[1,2]

[1]Department of Radiation Oncology, Fudan University Shanghai Cancer Center;
[2]Department of Oncology, Shanghai Medical College, Fudan University, Shanghai 200032, P.R. China

Received February 12, 2018; Accepted June 29, 2018

DOI: 10.3892/ijo.2018.4514

Abstract. Irinotecan, an analog of camptothecin, which is an inhibitor of topoisomerase I, is currently used in the treatment of metastatic colorectal cancer. Camptothecin derivatives have been demonstrated to exert radiosensitizing effects on several types of cancer cells. However, to date, at least to the best of our knowledge, few studies have examined these effects in colorectal cancer cell lines. In the present study, we examined the radiosensitizing effects of irinotecan on the p53-mutant colorectal cancer cell lines, HT29 and SW620, and explored the potential underlying mechanisms. Drug cytotoxicity tests revealed that the 24 h half-maximal inhibitory concentrations (IC_{50}s) of irinotecan as a single agent were 39.84 μg/ml (HT29 95% CI, 38.27-41.48) and 96.86 μg/ml (SW620 95% CI, 89.04-105.4); finally, concentrations <2 μg/ml were used in the subsequent experiments. Clonogenic assays revealed that irinotecan exerted radiosensitizing effects on the HT29 and SW620 cells, and the sensitivity enhancement ratios (SERs) at 2 Gy increased with increasing concentrations (SER at 2 Gy, 1.41 for the HT29 cells, 1.87 for the SW620 cells; with irinotecan at 2 μg/ml). Subsequently, the cells were divided into 4 groups: The control group, irinotecan group, radiation group and combination group. Compared with the control, irinotecan and radiation groups, the combination group had the slowest cell growth rate and the most obvious foci of ^{Ser139}p-γH2AX. Combined treatment resulted in a firstly decreased and then increased M phase arrest and led to the most significant G2/M phase arrest, followed by the most significant increase in apoptosis. The results of western blot analysis indicated that the expression levels of proteins related to the DNA damage response system (^{Ser1981}p-ATM, ^{Ser345}p-Chk1, ^{Thr68}p-Chk2 and ^{Ser139}p-γH2AX) and the cell cycle (^{Tyr15}p-Cdc2 and cyclin B1) exhibited the greatest increase in the combined group. In addition, the expression of ^{Ser216}p-Cdc25C was also increased in the combined group, indicating that irinotecan likely radiosensitized the p53-mutant HT29 and SW620 cells through the ATM/Chk/Cdc25C/Cdc2 pathway.

Introduction

Colorectal cancer is the second leading cause of cancer-related mortality in the United States (1). Pre-operative chemoradiotherapy (CRT), followed by total mesorectal excision, is the standard of care for patients with locally advanced rectal cancer (LARC) (2-4). The combination of radiation with capecitabine has been shown to significantly improve local control and local recurrence-free survival, but does not improve metastasis-free survival or overall survival (5). To acquire better outcomes, researchers have attempted to identify novel radiosensitizers, such as oxaliplatin, irinotecan and some molecular targeting agents (6). However, the addition of oxaliplatin, in addition to capecitabine, as a radiosensitizer has been demonstrated to have no benefit with regard to prognoses, but does show increased toxicity (7-10).

Irinotecan (also known as CPT-11), an analog of camptothecin (CPT), is currently used in the chemotherapy of metastatic colorectal cancer (11). The active form of irinotecan, SN-38, binds to and prevents topoisomerase I (TOP I) from rejoining transient DNA single-strand breaks (SSBs) during replication (12). Irinotecan-stabilized-TOP I-DNA complexes interact

Correspondence to: Professor Zhen Zhang, Department of Radiation Oncology, Fudan University Shanghai Cancer Center, 270 Dong An Road, Shanghai 200032, P.R. China
E-mail: zhen_zhang@fudan.edu.cn

*Contributed equally

Abbreviations: IC_{50}, half-maximal inhibitory concentration; SER, sensitivity enhancement ratio; DSB, double-strand breaks

Key words: irinotecan, radiosensitization, p53-mutant colorectal cancer cells, DNA damage response, cell cycle, cell apoptosis

with advancing replication forks during the S phase, convert SSBs into irreversible DNA double-strand breaks (DSBs) and result in cell death (13).

CPT derivatives exert radiosensitizing effects on various cell lines (14-17). However, to date, at least to the best of our knowledge, few studies have been published on these effects on colorectal cancer cell lines. A previous study found that CPT exerted radiosensitizing effects on p53-wild-type HCT116 colorectal cancer cells and proposed that p53 and p21 were the major cellular determinants for TOP I-mediated radiation sensitization (18). However, the radiosensitizing effects of irinotecan on p53-mutant colon cells remain unclear, and the potential mechanisms associated with the DNA damage response system, cell cycle arrest and cell apoptosis remain to be determined. Thus, in the present study, we examined the radiosensitizing effects of irinotecan on the p53-mutant colorectal cancer cell lines, HT29 and SW620, and explored the potential underlying mechanisms.

Materials and methods

Chemicals. Irinotecan was purchased from Jiangsu Hengrui Medicine Co., Ltd. (Jiangsu, China), dissolved in dimethyl sulfoxide to obtain a 100 mg/ml stock solution and stored at -20˚C.

Cell culture. The HT29 and SW620 cell lines were purchased from the Biochemistry and Cell Biology Institute of Shanghai, Chinese Academy of Sciences, within 3 months of the experiments. The HT29 cells were cultured in McCoy's 5A medium, and the SW620 cells were cultured in DMEM medium, both containing 10% heat-inactivated fetal bovine serum, 1% penicillin (final concentration, 100 U/ml) and streptomycin (final concentration, 0.1 mg/ml). The cells were maintained at 37˚C in a humidified atmosphere containing 5% CO_2. The experiments were conducted in the exponential phase of growth.

Cell viability assay. The HT29 ($8x10^3$) and SW620 ($8x10^3$) cells in 100 μl of culture medium were seeded onto 96-well plates (Corning Inc., Corning, NY, USA) and cultured overnight. The cells were treated with irinotecan by exchanging the medium premixed with various drug concentrations (0, 6.25, 12.5, 25, 50, 100, 200 and 400 μg/ml) for 24 h. Cell viability was evaluated using a Cell Counting kit-8 (CCK-8) assay (Dojindo Laboratories, Kumamoto, Japan), according to the manufacturer's instructions. The absorbance at 450 nm was then measured using a BioTek microplate reader and analyzed by Gen5 2.0 microplate software (BioTek Instruments, Inc., Winooski, VT, USA). The cell growth inhibition curve was presented, and the 24-h half-maximal inhibitory concentration (IC_{50}) of irinotecan was calculated. A chemotherapeutic drug exerts cytotoxic effects on cells, which can influence the accuracy of the results when it is combined with radiation. To examine the radiosensitizing effects of irinotecan, the concentrations need to be low in order to decrease the cytotoxic effects of the drug itself. According to past practice (19), low drug concentrations (<10% of the IC_{50} value or IC_{10} value) were considered for use in subsequent experiments. According to the IC_{50} values in this study (shown in the Results section below), low concentrations <4 μg/ml (0, 0.5, 1, 1.5, 2, 3 and 4 μg/ml) were used to examine the inhibitory effects of irinotecan as a single agent on clonogenic survival. Finally, we selected the doses of 0, 1 and 2 μg/ml as the experimental concentrations for use in combination with radiation.

Radiation exposure. The cells were irradiated with 6-MV X-rays using a linear accelerator (Varian Medical Systems, Palo Alto, CA, USA) at 3 Gy/min. Irradiation was performed at the Experimental Irradiation Core of the Fudan University Shanghai Cancer Center, Shanghai, China. In clonogenic assays, the cells were irradiated with X-rays at a dose of 0, 2, 4, 6 and 8 Gy. However, in the experiments comparing the results of the control, irinotecan, radiation and combined groups, there are no criteria on radiation doses. Preliminary experiments (data not shown) based on low radiation doses (2 and 4 Gy) revealed relatively small absolute values of the results and the differences among groups were not so obvious. In addition, preliminary experiments (data not shown) using high radiation doses (8-16 Gy) revealed severe toxicity of the radiation itself and it was hard to determine the differences between the radiation group and the combination group. Thus, we finally selected the dose of 6 Gy as the experimental radiation dose so that we could obtain obvious and high-quality results.

Clonogenic assay. A clonogenic assay is the standard method to examine the radiosensitizing effects of a drug. The cells were pre-seeded in 6-well plates (Corning Inc., Corning, NY, USA) at several densities (300-4,000 cells for the HT29 and 300-10,000 cells for the SW620 cells) overnight. After exchanging with drug-containing medium and incubation for 24 h, the cells were irradiated with X-rays at a series of dose levels (0, 2, 4, 6 and 8 Gy). The medium was then exchanged with culture medium without drugs, and the cells were incubated for 10 to 14 days to allow for colony formation. The colonies were fixed with 4% paraformaldehyde and stained with 0.1% crystal violet (100% methanol solution) prior to counting. The number of clones containing ≥50 cells was counted under a stereomicroscope (Leica Microsystems, Wetzlar, Germany). The plating efficiency (PE) was calculated in the following manner: PE = number of colonies formed without irradiation/number of cells inoculated x100%. The cell survival fraction (SF) was calculated at each irradiation dose in the following manner: SF = (number of colonies formed at a certain irradiation dose)/(number of cells inoculated x PE). SF curve fitting was conducted with a linear-quadratic model (20) via the equation $y = \exp[- (a \times x + b \times x^2)]$. Currently, the therapeutic regimen of 45-50 Gy/25-28 fractions (1.8-2.0 Gy per fraction) is widely used in the neoadjuvant chemoradiotherapy of locally advanced rectal cancers (21). In the present study, SFs at 2 Gy were used to determine the sensitivity enhancement ratio (SER), which was consistent with clinical radiotherapy. In this study, SER referred to the fractional ratio of counts of surviving colonies between cells treated with only 2 Gy X-rays compared to cells treated with both 2 Gy X-rays and irinotecan.

Cell growth assay. The HT29 ($4x10^3$) and SW620 ($3x10^3$) cells with 100 μl of culture medium were seeded onto 96-well plates (Corning Inc., Corning, New York, NY, USA) and cultured

overnight. After exchanging the medium with drug-containing medium and incubating for 24 h, the cells were irradiated with X-rays at 0 or 6 Gy. The medium was then exchanged with culture medium without drugs, and the cells were incubated for 5 days. The cell growth assay was performed daily using the CCK-8 assay kit as described above.

Cell cycle analysis. The HT29 and SW620 cells were seeded onto 60-mm plastic Petri dishes (Corning Inc.) and cultured overnight. After exchanging the medium with drug-containing medium and incubating the cells for 24 h, the cells were irradiated with X-rays at 0 or 6 Gy. The medium was then exchanged with culture medium without drugs, and cells were incubated for 3 and 24 h. The cells (discarding the culture medium) were harvested by trypsinization at 3 and 24 h following radiation. After rinsing 2 times with PBS, the cells were fixed with 75% ethanol at -20˚C overnight. The fixed cells were incubated in PBS for 15 min and subsequently stained with propidium iodide (PI) staining solution (50 μg/ml) for 30 min. The cell cycle was assayed with a flow cytometer (FACSCalibur; BD Biosciences, Franklin Lakes, NJ, USA) at an excitation wavelength of 488 nm and an emission wavelength of 585 nm and analyzed using BD CellQuest Pro software (643274 Rev. A; BD Biosciences). A doublet discrimination module was used when using flow cytometry to remove the doublets that can end up in the G2/M phase.

Cell apoptosis analysis. The HT29 and SW620 cells were seeded onto 60-mm plastic Petri dishes (Corning Inc.) and cultured overnight. After exchanging the medium with drug-containing medium and incubating the cells for 24 h, the cells were irradiated with X-rays at 0 or 6 Gy. The medium was then exchanged with culture medium without drugs, and the cells were incubated for 24 h to 3 days. The cells (including cells in the culture medium) were harvested by trypsinization at 24, 48 and 72 h following radiation. After rinsing twice with PBS, the cells were suspended in a binding buffer, stained with both 4 μl of PI and 4 μl of Annexin V-FITC per sample and loaded onto a flow cytometer (FACSCalibur; BD Biosciences) for FL1 (Annexin V) and FL2 (PI) bivariate analysis. Untreated samples stained with only PI or Annexin V-FITC were also prepared. The data from 20,000 cells/sample were collected, and the quadrants were set according to the population of viable, unstained cells in the untreated samples. The percentage of cells in the respective quadrants was calculated and analyzed using BD CellQuest Pro software (643274 Rev. A; BD Biosciences).

Immunofluorescence staining. A total of $5x10^4$ HT29 and SW620 cells were seeded separately onto 24-well plates (Corning Inc.) containing a glass coverslip in each well and cultured overnight. After exchanging the medium with drug-containing medium and incubating the cells for 24 h, the cells were irradiated with X-rays at 0 or 6 Gy. The medium was subsequently exchanged with culture medium without the drug, and cells were incubated for 24 h. The slides were then rinsed with PBS and fixed for 30 min in 4% paraformaldehyde. The cells were rinsed, treated with 1% Triton X-100 for permeabilization of the cell membrane, and rinsed again. The slides were blocked for 1 h in 5% bovine serum albumin (BSA) and finally incubated with phospho-histone H2A.X (Ser139) (20E3) rabbit monoclonal antibody (Alexa Fluor® 555 Conjugate; #8228S, diluted 1:100 in 5% BSA; Cell Signaling Technology, Danvers, MA, USA) at 4˚C overnight. The slides were rinsed, mounted with ProLong Diamond Antifade Mountant with DAPI (Thermo Fisher Scientific Inc., Waltham, MA, USA) and sealed. Images were aquired under a laser scanning confocal microscope (Leica Microsystems, Wetzlar, Germany). The numbers of ^{Ser139}p-γH2AX foci in the nuclei of at least 50 cells were counted in a double-blinded manner to calculate the average number of foci per nucleus.

Western blot analysis. The HT29 and SW620 cells were seeded onto 60-mm plastic Petri dishes (Corning Inc.) and cultured overnight. After exchanging the medium with drug-containing medium and incubating cells for 24 h, the cells were irradiated with X-rays at 0 or 6 Gy. The medium was then exchanged with culture medium without drugs, and cells were incubated for 3 and 24 h. The cells were lysed at 3 and 24 h following radiation with M-PER Mammalian Protein Extraction Reagent (Thermo Fisher Scientific Inc.) with the addition of protease inhibitors (cOmplete Tablets Mini; Roche, South San Francisco, CA, USA) and phosphatase inhibitors (PhosSTOP; Roche). Following the quantitation of the protein concentration using a Pierce BCA Protein Assay kit (Thermo Fisher Scientific Inc.) and protein degeneration at 100˚C for 10 min, the protein samples were resolved on SDS-polyacrylamide gels (^{Ser1981}p-ATM, ATM in 7.5% resolving gels, ^{Ser345}p-Chk1, Chk1, ^{Thr68}p-Chk2, Chk2, Cyclin B1, ^{Ser216}p-Cdc25C, Cdc25C, β-actin in 12.5% or 10% resolving gels, ^{Tyr15}p-Cdc2, Cdc2, ^{Ser139}p-γH2AX, ^{Ser10}p-Histone H3, Histone H3 in 12.5% resolving gels) by electrophoresis and subsequently transferred onto PVDF membranes (Millipore, Darmstadt, Germany). The membranes were blocked with 5% BSA and probed with primary antibodies at 4˚C overnight. The membranes were washed with Tris-buffered saline and Tween-20 (TBST) for 5x5 min, incubated with goat anti-mouse and goat anti-rabbit secondary antibodies for 1 h and washed again with TBST for 5x5 min. Antibodies against ^{Ser1981}p-ATM, ATM, ^{Ser345}p-Chk1 (#2348; dilution, 1:1,000), Chk1 (#2360; dilution, 1:1,000), ^{Thr68}p-Chk2 (#2197; dilution, 1:1,000), Chk2 (#6334; dilution, 1:1,000), ^{Ser139}p-γH2AX (#9718; dilution, 1:1,000), ^{Ser216}p-Cdc25C (#4901; dilution, 1:1,000), Cdc25C (#4688; dilution, 1:1,000), ^{Tyr15}p-Cdc2 (#4539; dilution, 1:1,000), Cdc2 (#9116; dilution, 1:1,000), cyclin B1 (#12231; dilution, 1:1,000), ^{Ser10}p-Histone H3 (#53348; dilution, 1:1,000), Histone H3 (#4499; dilution, 1:1,000) and β-actin, as well as goat anti-mouse (#7056; dilution, 1:10,000) and goat anti-rabbit (#7074; dilution, 1:10,000) secondary antibodies were purchased from Cell Signaling Technology (Cell Signaling Technology). The protein bands were visualized using an enhanced chemiluminescence detection system (Thermo Fisher Scientific Inc.). Protein bands were analyzed by ImageJ software version 1.8.0 (National Institutes of Health, Bethesda, MD, USA).

Statistical analysis. All experiments were repeated independently at least 3 times. SPSS version 22.0 software (SPSS Inc., Chicago, IL, USA) was used for the statistical analysis. The data are presented as the means ± standard deviation. Comparisons among multiple groups were conducted using

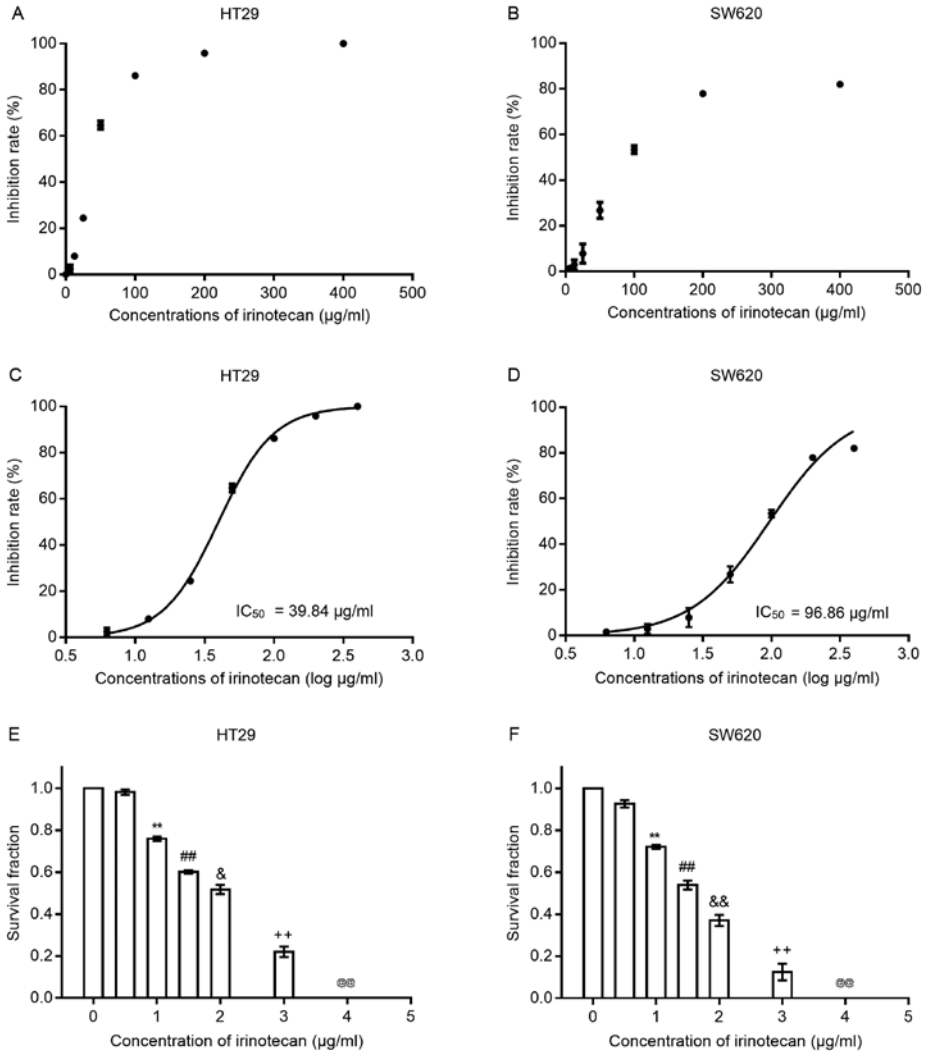

Figure 1. Drug cytotoxicity tests of irinotecan as a single agent. Drug inhibition scatter grams in (A) HT29 and (B) SW620 cells were obtained through CCK-8 assays. Also, 24 h IC_{50} values of irinotecan for (C) HT29 and (D) SW620 were calculated from drug inhibition curves with log transformed concentrations (log μg/ml). The inhibitory effects of irinotecan at low concentrations (<10% of the IC_{50}) on the clonogenic survival of (E) HT29 and (F) SW620 cells were then measured through clonogenic assays. Error bars represent the means ± SD of at least n=3 determinations. **P<0.01 vs. irinotecan (0.5 μg/ml) group. $^{\#\#}$P<0.01 vs. irinotecan (1.0 μg/ml) group. $^{\&}$P<0.05 vs. irinotecan (1.5 μg/ml) group. $^{\&\&}$P<0.01 vs. irinotecan (1.5 μg/ml) group. $^{++}$P<0.01 vs. irinotecan (2.0 μg/ml) group. $^{@@}$P<0.01 vs. irinotecan (3.0 μg/ml) group. IC_{50}, half-maximal inhibitory concentration. SD, standard deviation.

the one-way ANOVA or two-way ANOVA method for quantitative data. Turkey's test was used for the post hoc multiple comparisons. A P-value <0.05 was considered to indicate a statistically significant difference. All curves and plots were generated using GraphPad Prism 7.0 software (GraphPad Software Inc., San Diego, CA, USA).

Results

Irinotecan inhibits the viability and proliferation of HT29 and SW620 cells. To verify the cytotoxic effects of irinotecan on colorectal cancer cells, we first treated both cell lines with irinotecan as a single agent at several increasing concentrations (0, 6.25, 12.5, 25, 50, 100, 200 and 400 μg/ml) for 24 h. Cell viability was examined using the CCK-8 assay kit. As the scatter grams shown in Fig. 1 A and B, the inhibition rates increased with the increasing drug concentration (0, 6.25, 12.5, 25, 50, 100, 200 and 400 μg/ml) in both cell lines; the HT29 cells seemed to be more sensitive to irinotecan than the SW620 cells. We then transformed the drug concentrations into log μg/ml style. The drug inhibition curves (shown in Fig. 1C and D) exhibited an S-like shape, from which IC_{50} values at 24 h for both cell lines were calculated. For the HT29 cells, the IC_{50} value was 39.84 μg/ml (95% CI, 38.27-41.48) and for the SW620 cells, it was 96.86 μg/ml (95% CI, 89.04-105.4). Concentrations of irinotecan <10% of the IC_{50} value were considered for use in the subsequent experiments.

Subsequently, we examined the inhibitory effects of irinotecan on clonogenic survival at low concentrations (0, 0.5, 1, 1.5, 2, 3 and 4 μg/ml) for 24 h (Fig. 1E and F). The results revealed that the clonogenic survival rates were very low when the concentration was >2 μg/ml; thus, we selected the dose of 0, 1 and 2 μg/ml as the experimental concentrations for use in combination with radiation.

Low concentrations of irinotecan induce a DNA damage response and G2/M arrest, with minimal apoptosis. Both cell lines were treated with low concentrations of irinotecan (0, 1

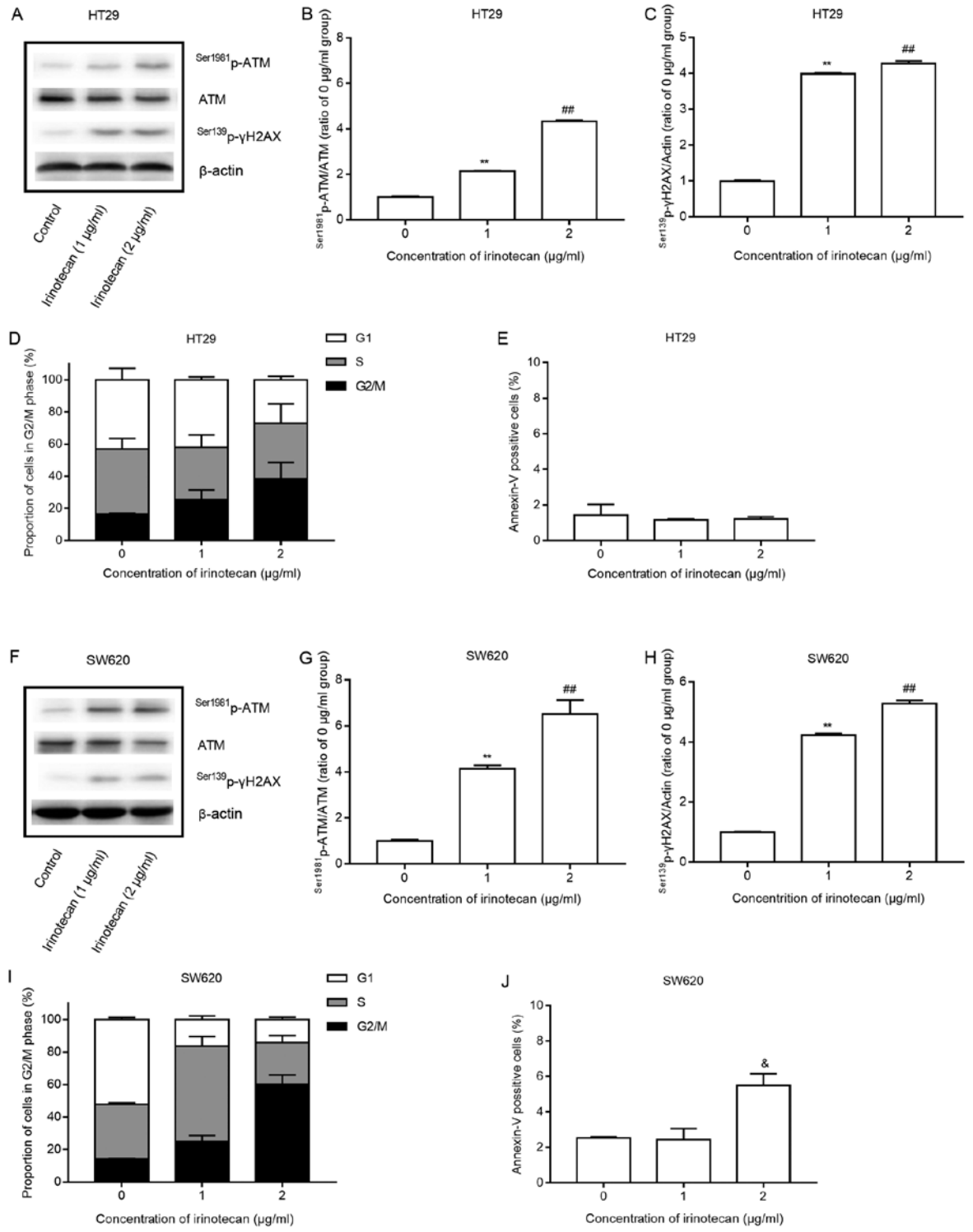

Figure 2. Low concentrations (0, 1 and 2 μg/ml) of irinotecan as a single agent induce DNA damage response and G2/M arrest, with minimal apoptosis. (A and F) Expression of ^{Ser1981}p-ATM, ATM and ^{Ser139}p-γH2AX in HT29 and SW620 cells. (B and G) Ratio of ^{Ser1981}p-ATM to ATM in HT29 and SW620 cells. (C and H) Ratio of ^{Ser139}p-γH2AX to actin in HT29 and SW620 cells. (D and I) Distribution of G1, S and G2/M phases in HT29 and SW620 cells. (E and J) Changes in cell apoptosis of HT29 and SW620 cells. Error bars represent the means ± SD of at least n=3 determinations. **P<0.01 vs. irinotecan (0 μg/ml) group and $^{\#\#}$P<0.01 vs. irinotecan (1 μg/ml) group in HT29 and SW620 cells. $^{\&}$P<0.05 vs. irinotecan (1 μg/ml) group in SW620 cells. SD, standard deviation.

and 2 μg/ml) as a single agent. The cells were harvested after 24 h of incubation with irinotecan, and the protein expression of ^{Ser1981}p-ATM, ATM and ^{Ser139}p-γH2AX was measured by western blot analysis. The cells were also submitted to flow cytometry to analyze changes in the cell cycle and apoptosis.

Low levels of irinotecan induced a statistically significant increase in the expression of ^{Ser1981}p-ATM/ATM and ^{Ser139}p-γH2AX (Fig. 2 A-C and F-H) and a marked increase in the proportion of cells in the G2/M phase, with a corresponding decrease in the proportion of cells in the G1 phase, all in a

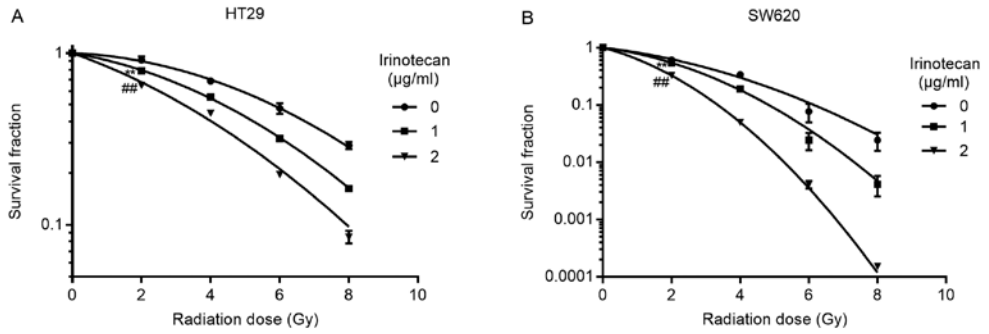

Figure 3. Irinotecan sensitizes the HT29 and SW620 cells to radiation. The clonogenic curves of (A) HT29 and (B) SW620 cells were obtained through clonogenic assays (irinotecan, 0, 1 and 2 μg/ml; radiation, 0-8 Gy). Error bars represent the means ± SD of at least n=3 determinations. **P<0.01 vs. irinotecan (0 μg/ml) group. $^{\#\#}$P<0.01 vs. irinotecan (1 μg/ml) group. SD, standard deviation.

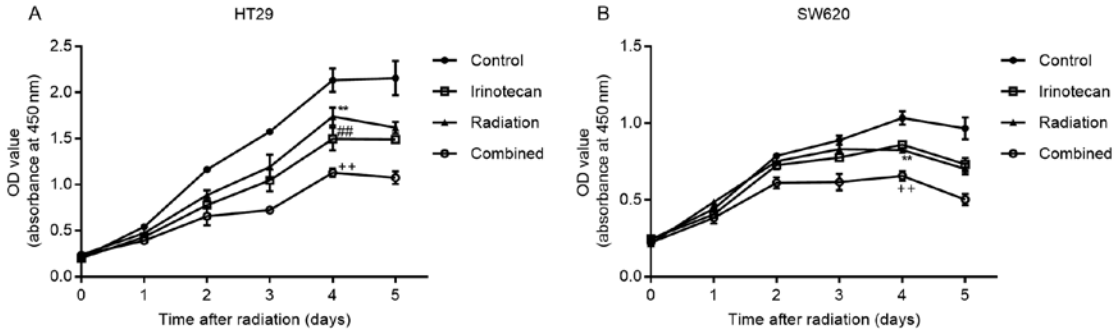

Figure 4. Irinotecan combined with radiation resulted in the slowest cell growth. (A and B) The cell growth curves of HT29 and SW620 cells were obtained through CCK-8 assays over 5 consecutive days following treatment (irinotecan, 0 and 2 μg/ml; radiation, 0 and 6 Gy). Error bars represent the means ± SD of at least n=3 determinations. **P<0.01 vs. control group. $^{\#\#}$P<0.01 vs. radiation group. $^{++}$P<0.01 vs. irinotecan group. SD, standard deviation. Combined, refers to the combination group.

concentration-dependent manner (Fig. 2D and I). The results indicated that SW620 cells were more sensitive to delay at the G2/M phase than the HT29 cells. However, only a significant increase (P=0.022, 2 μg/ml vs. 1 μg/ml) in apoptosis was detected at 2 μg/ml in the SW620 cells and no increase was detected in the HT29 cells after 24 h of irinotecan treatment (Fig. 2E and J).

These findings suggest that irinotecan activates the DNA damage response system, induces potent G2/M phase arrest and minimal apoptosis of the HT29 and SW620 cells, consistent with the findings of previous studies (22,23). These changes may potentially represent important mechanisms for radiosensitization.

Irinotecan sensitizes the HT29 and SW620 cells to radiation. We selected 1 and 2 μg/ml of irinotecan for use in the radiosensitization experiments. The cells were treated with irinotecan for 24 h, followed by treatment with radiation at different doses of up to 8 Gy. The culture medium was then exchanged with irinotecan-free medium for 10-14 days to enable colony formation. Following linear-quadratic analysis (LQ model), we found that irinotecan effectively sensitized the HT29 and SW620 cells to radiation, and the SER at 2 Gy increased with the increasing drug concentration. For the HT29 cells, the SER at 2 Gy was 1.16 and 1.41 at 1 and 2 μg/ml, respectively, and for the SW620 cells, the SER at 2 Gy was 1.13 and 1.87 at 1 and 2 μg/ml, respectively (Fig. 3). Thus, we concluded that irinotecan is a good radiosensitizer against p53-mutant colorectal cancer cells.

Subsequently, we verified the radiosensitizing effects of irinotecan by drawing cell growth curves. The cells were incubated for 5 days following 24 h of drug treatment, followed by radiation treatment. Cell viability was measured daily using the CCK-8 assay kit. As expected, irinotecan in combination with radiation resulted in a reduced growth of both the HT29 and SW620 cells compared with growth in the irinotecan, radiation and control groups, with most high significance observed on days 4 and 5 (Fig. 4).

The radiosensitizing effects of irinotecan are associated with the activation of the DNA damage response. The cells were treated with irinotecan (2 μg/ml), radiation (6 Gy) or irinotecan (2 μg/ml) in combination with radiation (6 Gy). The formation of ^{Ser139}p-γH2AX foci was illustrated by immunofluorescence staining. Subsequently, the expression levels of proteins related to the DNA damage response, such as ^{Ser1981}p-ATM, ATM, ^{Ser345}p-Chk1, Chk1, ^{Thr68}p-Chk2, Chk2 and ^{Ser139}p-γH2AX, were measured by western blot analysis.

The results of immunofluorescence microscopy revealed that the ^{Ser139}p-γH2AX foci in the nuclei of both the HT29 and SW620 cells at 24 h following radiation were the most obvious in the combination group. The immunofluorescence staining images of the HT29 cells are presented in Fig. 5; however, the images of the SW620 cells are not presented (data not shown).

The results of western blot analysis also verified these findings. Compared with results from the irinotecan and radiation groups, irinotecan in combination with radiation resulted

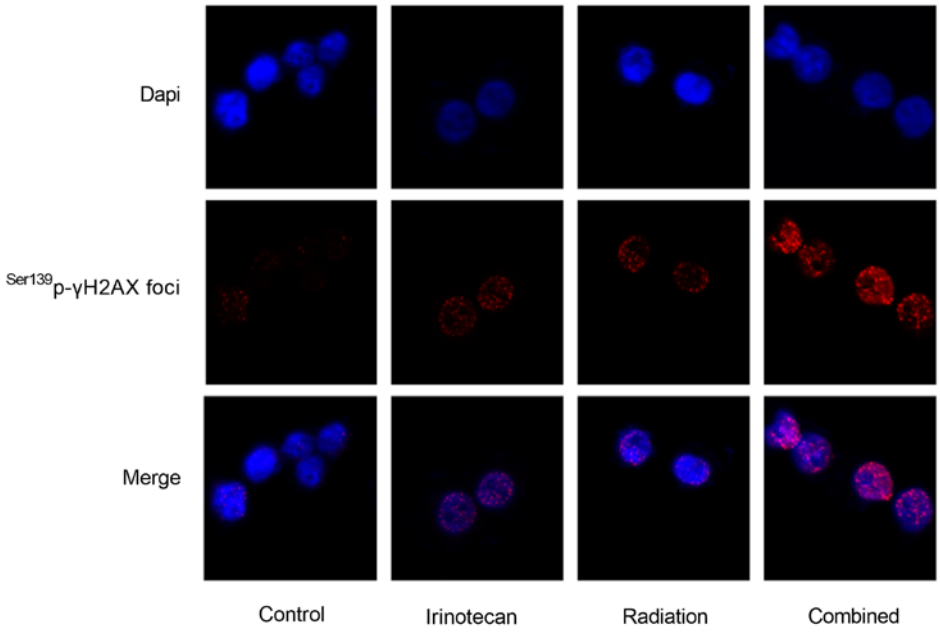

Figure 5. Irinotecan combined with radiation results in the most obvious γH2AX foci. Foci of ^{Ser139}p-γH2AX in HT29 cells are illustrated by immunofluorescence staining at 24 h following treatment (irinotecan, 0 and 2 μg/ml; radiation, 0 and 6 Gy).

in a marked increase in the phosphorylation levels of ATM at Ser1981 and γH2AX at Ser139 at 3 and 24 h. Combined treatment also increased the activation of Chk1 at Ser345 and Chk2 at Thr68 at 3 h, with significantly increased ratios of ^{Ser1981}p-ATM/ATM, ^{Ser345}p-Chk1/Chk1 and ^{Thr68}p-Chk2/Chk2, and the activation of these proteins persisted for >24 h (Fig. 6A-E and F-J). These results indicate that irinotecan could likely enhance radiation-induced DNA double-strand damage and the DNA damage response process through the ATM/Chk signaling pathway.

The radiosensitizing effects of irinotecan are attributable to an enhanced G2/M phase arrest. The cells were treated with irinotecan (2 μg/ml), radiation (6 Gy) or irinotecan (2 μg/ml) combined with radiation (6 Gy). The cell cycle distribution was measured by flow cytometry at 3 and 24 h following radiation. Subsequently, the expression of levels proteins related to G2/M phase arrest, such as ^{Tyr15}p-Cdc2, Cdc2 and cyclin B1, were measured by western blot analysis.

The proportions of cells in the G2/M phase were elevated to a fairly high level following pre-treatment with irinotecan. Cells in the G2/M phase are more sensitive to radiation (24). Thus, it was suggested that treatment with irinotecan prior to radiation could produce a greater number of radiosensitized cells.

At 3 h following radiation, the combination group exhibited a slight increase in the number of cells undergoing G2/M phase arrest compared with the irinotecan group (data not shown). However, 24 h later, a marked increase in the number of cells undergoing G2/M phase arrest was observed in the radiation group and the combination group, indicating that it took some time for radiation to induce cell cycle arrest. As expected, the combination group exhibited the highest rates of G2/M phase arrest at 24 h when compared with those in the other 3 groups. The rates of G2/M phase arrest were 66.08±1.42% for the HT29 cells and 79.35±1.49% for the SW620 cells, indicating that the addition of irinotecan enhanced the activation of the cell cycle checkpoint and delayed the growth of the cells. The cell cycle distributions at 24 h are presented in Fig. 7A and B.

Cdc2 and cyclin B1 are two key regulators of the G2-to-M phase transition. We found a significant increase in the expression levels of ^{Tyr15}p-Cdc2 (and in the ratio of ^{Tyr15}p-Cdc2/Cdc2) and cyclin B1 at 3 h in the combination group compared with values in the other 3 groups, and this increase was enhanced over 24 h (Fig. 7C-E and F-H).

The radiosensitizing effects of irinotecan are associated with the ATM/Chk/Cdc25C/Cdc2 pathway in p53-mutant colorectal cancer cells. The tumor suppressor p53 is a key protein in checkpoint pathways in normal cells, and the mutation of the p53 gene is considered an important step in colorectal cancer formation. There are two pathways related to G2/M phase arrest, the p21-dependent pathway in p53-wild-type cancer cells and the Chk-dependent pathway in p53-deficient cancer cells (24-27). For p53-mutant HT29 and SW620 cells, we hypothesized that the Chk-dependent pathway plays an important role in irinotecan-induced or/and radiation-induced G2/M phase arrest. The key intermediate factor between Chk proteins and the Cdc2-cyclin B1 complex is Cdc25. The negative regulation of Cdc25C by phosphorylation at Ser216 can subsequently inhibit the activity of the Cdc2-cyclin B1 complex and lead to G2/M phase arrest. Therefore, we examined the effects of irinotecan and radiation on the expression of ^{Ser216}p-Cdc25C and Cdc25C in p53-mutant HT29 and SW620 cells.

As shown in Fig. 8A and B, and C and D, for both cell lines, irinotecan and radiation as single treatments slightly increased the expression of ^{Ser216}p-Cdc25C; however, combined treatment significantly enhanced phosphorylation, with an increasing ratio of p-Cdc25C/Cdc25C. These results suggest that the addition of irinotecan to radiation treatment promotes cycle arrest through the negative regulation of Cdc25C by phosphorylation at Ser216, and the ATM/Chk/Cdc25C/Cdc2/

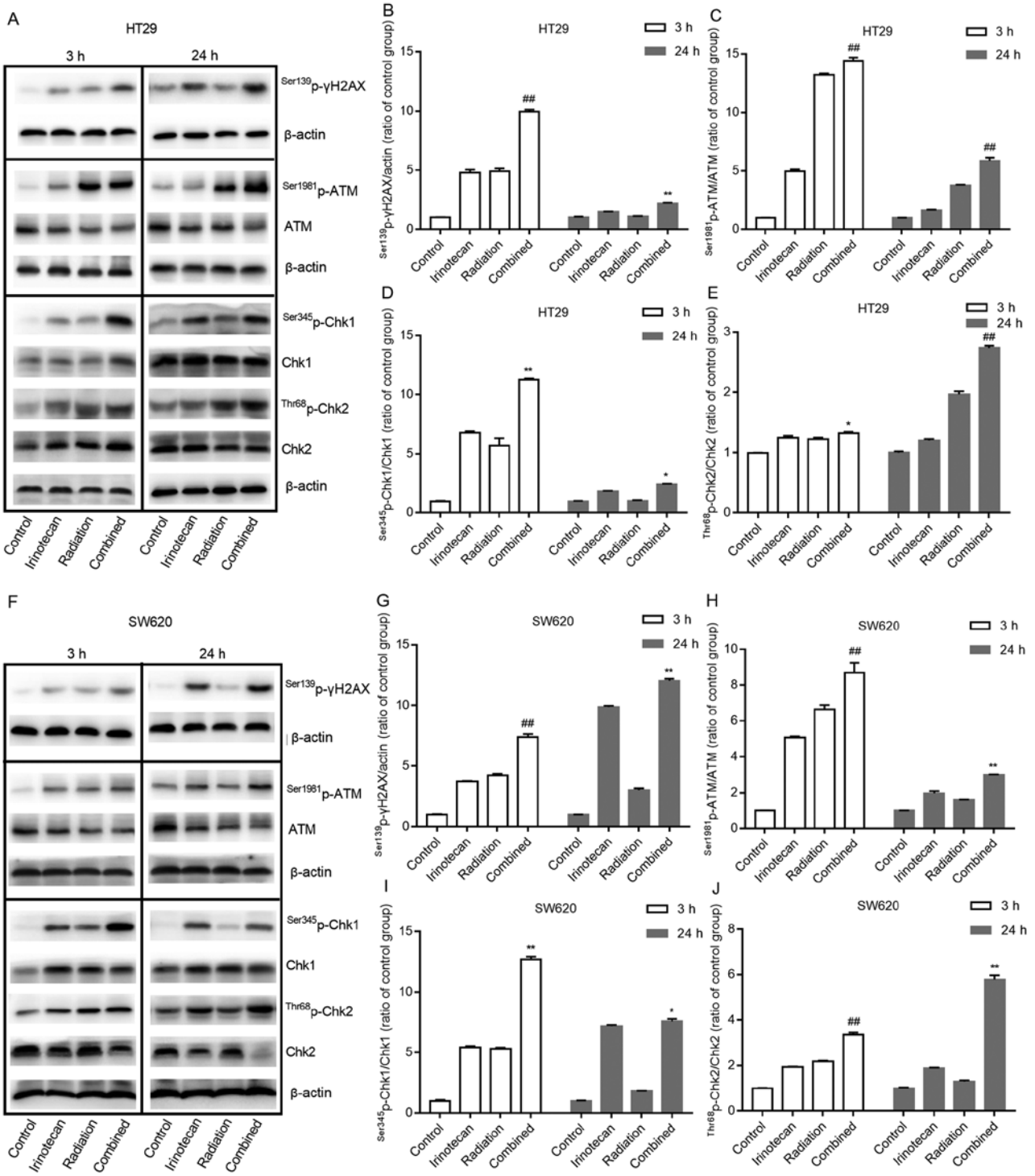

Figure 6. Irinotecan combined with radiation results in the most obvious activation of the DNA damage response. (A and F) Expression of ^{Ser139}p-γH2AX, ^{Ser1981}p-ATM, ATM, ^{Ser345}p-Chk1, Chk1, ^{Thr68}p-Chk2 and Chk2 in HT29 and SW620 cells at 3 and 24 h following treatment (irinotecan, 0 and 2 μg/ml; radiation, 0 and 6 Gy). (B and G) Ratio of ^{Ser139}p-γH2AX to actin in HT29 and SW620 cells. (C and H) Ratio of ^{Ser1981}p-ATM to ATM in HT29 and SW620 cells. (D and I) Ratio of ^{Ser345}p-Chk1 to Chk1 in HT29 and SW620 cells. (E and J) Ratio of ^{Thr68}p-Chk2 to Chk2 in HT29 and SW620 cells. Error bars represent the means ± SD of at least n=3 determinations. *P<0.05 vs. irinotecan group. **P<0.01 vs. irinotecan group. $^{\#\#}$P<0.01 vs. radiation group. SD, standard deviation. Combined, refers to the combination group.

cyclin B1 pathway likely plays an important role in the mechanism of G2/M phase arrest.

Radiosensitization by irinotecan results in a decreased and then increased M phase arrest. Histone H3 phosphorylation is a well-established marker of mitosis (28). In this study, to determine whether radiation combined with irinotecan causes the arrest of cells in the G2 phase or M phase, we examined the expression of ^{Ser10}p-Histone H3 at 3 h and 24 h following treatment.

As shown in Fig. 9A and B, and C and D, for both cell lines, the cells in the control group exhibited some degree

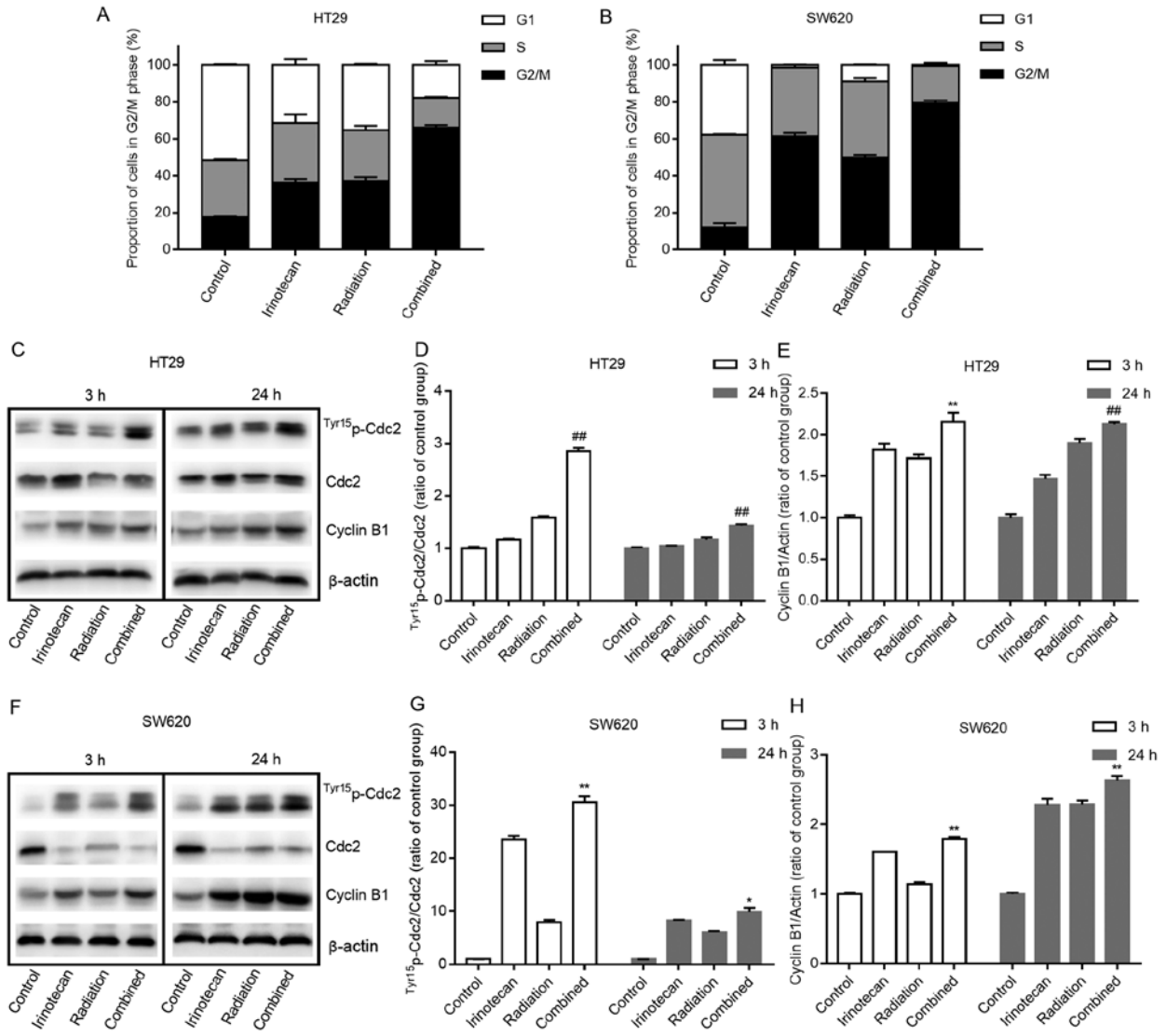

Figure 7. Irinotecan in combination with radiation results in the greatest degree of G2/M arrest. (A and B) Distribution of G1, S and G2/M phases in HT29 and SW620 cells at 24 h following treatment (irinotecan, 0 and 2 μg/ml; radiation, 0 and 6 Gy). (C and F) Expression of ^{Tyr15}p-Cdc2, Cdc2 and cyclin B1 in HT29 and SW620 cells at 3 and 24 h following treatment (irinotecan, 0 and 2 μg/ml; radiation, 0 and 6 Gy). (D and G) Ratio of ^{Tyr15}p-Cdc2 to Cdc2 in HT29 and SW620 cells. (E and H) Ratio of cyclin B1 to actin in HT29 and SW620 cells. Error bars represent the means ± SD of at least n=3 determinations. *P<0.05 vs. irinotecan group. **P<0.01 vs. irinotecan group. $^{\#\#}$P<0.01 vs. radiation group. SD, standard deviation. Combined, refers to the combination group.

of expression of ^{Ser10}p-Histone H3. Of note, the effects of irinotecan alone on the HT29 cells and SW620 cells were not consistent. For the HT29 cells, irinotecan alone led to an enhanced expression of ^{Ser10}p-Histone H3 at 3 and 24 h. However, for the SW620 cells, irinotecan alone reduced the expression of ^{Ser10}p-Histone H3 at 3 h and lasted for >24 h.

For both cell lines, treatment with radiation alone inhibited the expression of ^{Ser10}p-Histone H3 for a short period of time, showing a low-level expression of ^{Ser10}p-Histone H3 at 3 h. However, its expression increased in the following 24 h, showing an increased level at 24 h after treatment. When radiation was combined with irinotecan, we found the same trend at 3 and 24 h following combined treatment. For the SW620 cells, the expression of ^{Ser10}p-Histone H3 in the combination group at 24 h was higher than that in the irinotecan, radiation and control groups. However, for the HT29 cells, the expression of ^{Ser10}p-Histone H3 in the combination group at 24 h was lower than that in the radiation group, but higher than that in the irinotecan and control group. However, the expression of ^{Ser10}p-Histone H3 in the combination group exhibited an increasing trend, probably exceeding the radiation group in the following hours. Thus, we found that irinotecan in combination with radiation resulted in a decreased and then increased M phase arrest.

The radiosensitizing effects of irinotecan are attributable to enhanced apoptosis following the cycle arrest of p53-mutant colorectal cancer cells. It has been previously demonstrated that the DNA damage induced by the TOP I inhibitor, irinotecan, triggers the long-term cell cycle arrest of p53-wild-type colorectal carcinoma cells and transient arrest followed by apoptosis in p53-mutant cells (29). Thus, for the two p53-mutant cell lines used in the present study, we examined whether the G2/M phase arrest caused by irinotecan and radiation was followed by apoptosis.

The cells were treated with irinotecan (2 μg/ml), radiation (6 Gy) or irinotecan (2 μg/ml) in combination with radiation

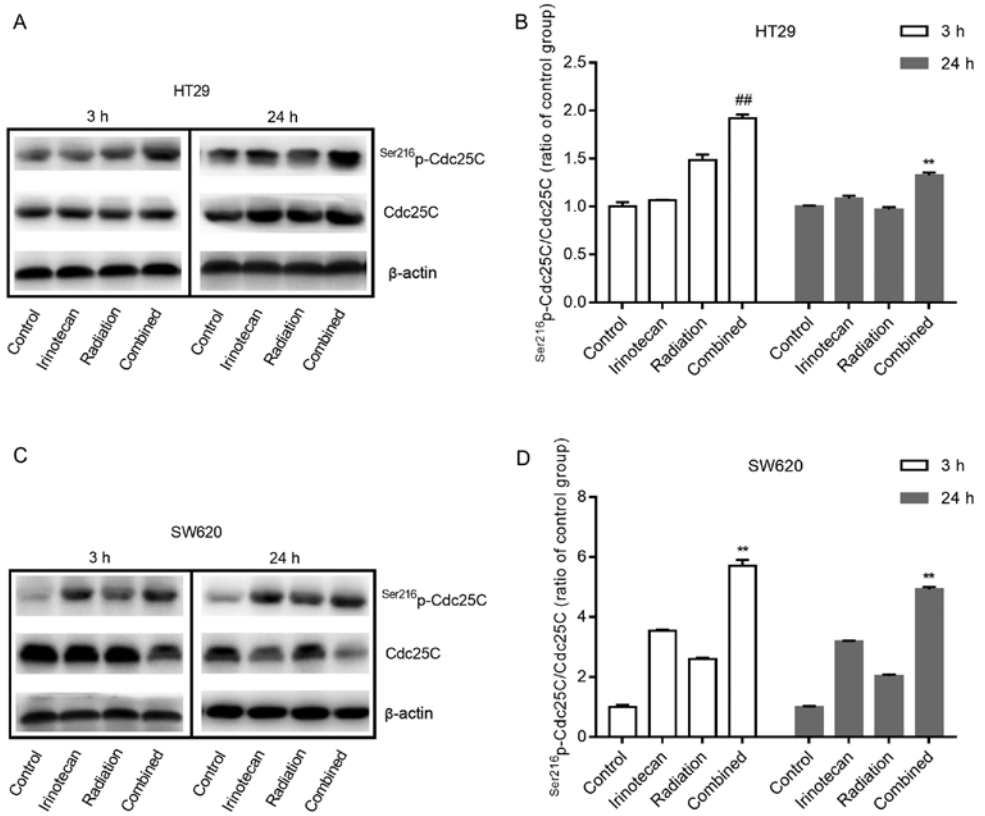

Figure 8. Radiosensitizing effects of irinotecan are associated with increased ^{ser216}p-Cdc25C expression in p53-mutant colorectal cancer cells. (A and C) Expression of ^{Ser216}p-Cdc25C and Cdc25C in HT29 and SW620 cells at 3 and 24 h following treatment (irinotecan, 0 and 2 μg/ml; radiation, 0 and 6 Gy). (B and D) Ratio of ^{Ser216}p-Cdc25C to Cdc25C in HT29 and SW620 cells. Error bars represent the means ± SD of at least n=3 determinations. **P<0.01 vs. irinotecan group. $^{\#\#}$P<0.01 vs. radiation group. SD, standard deviation. Combined, refers to the combination group.

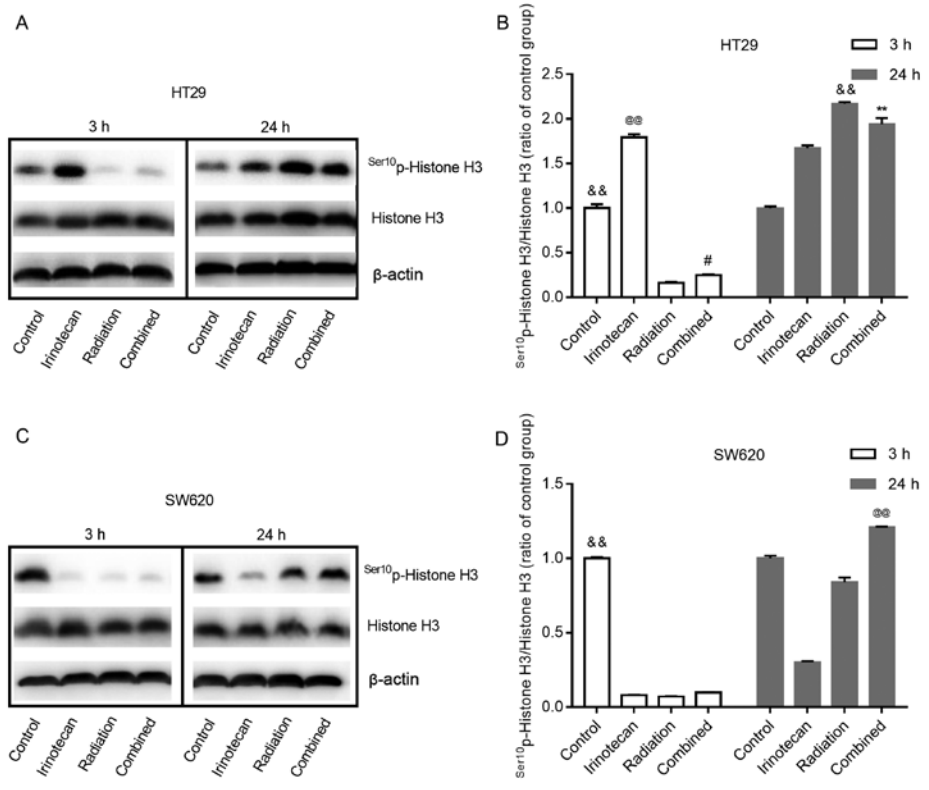

Figure 9. Irinotecan in combination with radiation results in a decreased and then increased M phase arrest. (A and C) Expression of ^{Ser10}p-Histone H3 and Histone H3 in HT29 and SW620 cells at 3 and 24 h following treatment (irinotecan, 0 and 2 μg/ml; radiation, 0 and 6 Gy). (B and D) Ratio of ^{Ser10}p-Histone H3 to Histone H3 in HT29 and SW620 cells. Error bars represent the means ± SD of at least n=3 determinations. $^{@@}$P<0.01 vs. control group, $^{\&\&}$P<0.01 vs. combination group, $^{\#}$P<0.05 vs. radiation group and **P<0.01 vs. irinotecan group. SD, standard deviation. Combined, refers to the combination group.

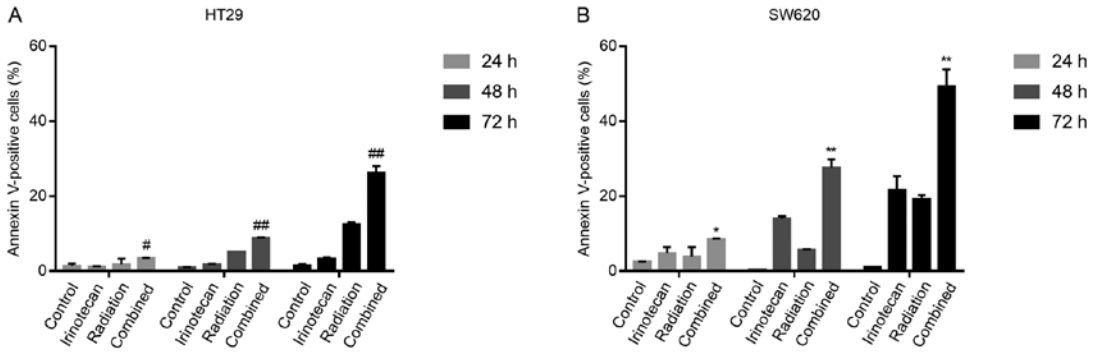

Figure 10. Irinotecan in combination with radiation results in the most significant increase in apoptosis after G2/M phase arrest in p53-mutant colorectal cancer cells. (A and B) The rates of apoptosis in HT29 and SW620 cells at 24, 48 and 7 h following treatment (irinotecan, 0 and 2 μg/ml; radiation, 0 and 6 Gy). Error bars represent the means ± SD of at least n=3 determinations. $^{\#}$P<0.05 vs. irinotecan group in HT29 cells. $^{\#\#}$P<0.01 vs. radiation group in HT29 cells. *P<0.05 vs. control group in SW620 cells. **P<0.01 vs. irinotecan group in SW620 cells. SD, standard deviation. Combined, refers to the combination group.

(6 Gy). Cell apoptosis was measured by flow cytometry at a series of time points (24, 48 and 72 h) following radiation.

As expected, the rates of cell apoptosis were highest in the combination group, compared with the control group, irinotecan group and radiation group. However, at 24 h, the rates of apoptosis were relatively low and increased significantly when the cells were incubated for a further 24 or 48 h. The rates of apoptosis at 7 h were 26.25±1.77% for the HT29 and 49.40±4.45% for the SW620 cells (Fig. 10). Thus, the radiosensitizing effects of irinotecan are attributable to short-term DNA damage-induced G2/M cycle arrest, followed by enhanced apoptosis, which significantly inhibits cell viability and proliferation.

Discussion

Colorectal cancer is the second leading cause of cancer-related mortality in the United States (1). For patients with LARC, pre-operative CRT followed by total mesorectal excision is the standard treatment according to the NCCN Clinical Practice Guidelines in Oncology Rectal Cancer Version 2.2018 (21). The combined use of radiation with capecitabine has been shown to achieve a pathologically complete response in 15 to 25% of cases and to result in downstaging in 50 to 60% of cases (30). Researchers have attempted to identify novel radiosensitizers to achieve better outcomes, and the addition of oxaliplatin, in addition to capecitabine, as a radiosensitizer has been demonstrated to have no benefit with regard to prognosis and resulted in increased toxicity (7-10). Thus, other radiosensitizing agents are required.

Irinotecan (also known as CPT-11), an analog of CPT, which is an inhibitor of TOP I, is currently used in the chemotherapy of metastatic colorectal cancer. The active form of irinotecan, SN-38, can bind to and prevent TOP I from rejoining transient DNA breaks during DNA replication, RNA transcription and DNA damage repair, transforming the concealed 'potentially sublethal' DNA damage into 'sublethal' DNA damage (13). TOP I inhibitors exhibit S-phase-specific cytotoxicity, which has been explained by the 'Folk Collision Model'; according to Chen *et al* (31). It is hypothesized that the collision between the replication machinery and the drug-trapped TOP I cleavable complex leads to eventual G2-phase cell cycle arrest and cell death (32), and the addition of radiation can convert this 'sublethal' DNA damage into 'lethal' DNA damage.

In previous studies, CPT derivatives were demonstrated to exert radiosensitizing effects on many cell types (14-17). Chen *et al* demonstrated that CPT derivatives radiosensitized human breast cancer MCF-7 cells when drug treatments were administered prior to, but not following, radiation (33). However, few studies have been published on the effects on colorectal cancer cell lines. Chen *et al* (18) found that CPT exerted radiosensitizing effects on parental HCT116 colorectal cancer cells, with an SER of 2.0. Omura *et al* demonstrated radiosensitization with SN-38 in HT29 spheroids (34).

The molecular mechanisms of the radiosensitization of TOP I inhibitors are largely unknown. Chen *et al* proposed that the drug-trapped TOP I cleavable complex may initiate TOP I-mediated radiosensitization by 'interacting' with the replication fork during active DNA synthesis, leading to at least three major biochemical events, including DNA DSBs, replication fork arrest and an aborted 'cleaved' TOP I-DNA complex (31). The induction of TOP I-mediated radiosensitization likely requires one or more of these three events.

When DNA damage occurs, a variety of kinases are activated and connect the checkpoint with the cell cycle machinery. The activation of the DNA damage checkpoint, involving ATM kinase activation and ATM autophosphorylation at Ser1981, can lead to cell cycle arrest to prevent mitosis in the presence of damaged DNA. G2/M phase arrest delays the proliferation of cancer cells, and cells in the G2/M phase are more sensitive to radiation (24). Thus, the G2/M transition is considered a specific target, and this arrest may be a useful strategy in CRT.

In this study, we found that low levels of irinotecan led to a certain degree of activation of the DNA damage response, followed by a marked increase in the number of cells undergoing G2/M phase arrest, inducing the transformation of many cells into a more radiosensitive status. Radiation also results in DNA DSBs in cells, followed by G2/M phase arrest and apoptosis. Thus, the addition of low concentrations of irinotecan as a sensitizer to radiation treatment may be feasible.

The tumor suppressor p53 is one of the key proteins in checkpoint pathways (26). The activation of p53 may lead to growth arrest at both the G1 and G2/M phases. In the canonical p53-dependent G2/M phase arrest pathway, overexpressed p53 binds to the promoter of the p21 Cdk inhibitor, causing p21 to accumulate. The resulting inhibition of Cdc2-cyclin B1

activity leads to cell cycle arrest. However, several studies have indicated that the absence of p53 (via mutation or deficiency) is sufficient to induce G2/M arrest, and this pathway is switched from p21-dependent to Chk-dependent in p53-deficient cells (24,25,35).

At the G2/M transition, the removal of inhibitory phosphorylation at Thr14 and Tyr15 results in Cdc2 activation, and this reaction is mediated by Cdc25 phosphatases (36). In the Chk-dependent pathway, in response to DNA damage, activated ATM phosphorylates/activates Chk1 at Ser345 and Chk2 at Thr68 (37). The two phosphorylated Chk proteins subsequently phosphorylate Cdc25C at Ser216, leading to the binding of 14-3-3 proteins and the sequestration of Cdc25C in the cytoplasm, inactivating the phosphatase activity of Cdc25C. The negative regulation of Cdc25C by phosphorylation at Ser216 can subsequently inhibit the activity of the Cdc2-cyclin B1 complex and lead to G2/M phase arrest, which is an important regulatory mechanism used by cells to block mitotic entry in response to DNA damage.

As for the mechanisms responsible for the radiosensitizing effects induced by CPT derivatives, few studies have examined the signaling pathways associated with the DNA damage response system, the cell cycle and apoptosis. Chen *et al* (18) demonstrated that the SERs decreased from 2.0 in p53-wild-type HCT-116 cells to 1.6 in HCT-116 ($p53^{-/-}$) cells and to 1.0 in HCT-116 ($p21^{-/-}$) cells. These findings indicated that TOP I-mediated sublethal damage may activate DNA damage responses, including p53 and p21 regulatory pathways, and eventually lead to radiosensitization.

In the present study, both the HT29 and SW620 were p53-mutant cell lines. Irinotecan exerted a radiosensitizing effect on the HT29 and SW620 cells, and the SERs increased with increasing drug concentration (SER at 2 Gy, 1.41 for the HT29 cells; SER at 2 Gy, 1.87 for the SW620 cells, with irinotecan at 2 μg/ml). Compared with the control group, the irinotecan group and radiation group, the combination group exhibited the slowest cell growth rate and the most obvious foci of ^{Ser139}p-γH2AX. Combined treatment resulted in the most significant G2/M phase arrest, and the effects lasted for >24 h, followed by the most significant increase in apoptosis. The results of western blot analysis indicated that the expression of proteins related to the DNA damage response system (^{Ser1981}p-ATM, ^{Ser345}p-Chk1, ^{Thr68}p-Chk2, ^{Ser139}p-γH2AX), as well as of those related to the cell cycle (^{Tyr15}p-Cdc2, cyclin B1), was increased in the combination group. We propose that in p53-mutant colorectal cancer cells, the mechanism for G2/M phase arrest of radiosensitization is Chk-dependent and that Cdc25C is involved. As expected, the expression of ^{Ser216}p-Cdc25C was also increased in the combination group, indicating that irinotecan likely radiosensitized the p53-mutant HT29 and SW620 cells through the ATM/Chk/Cdc25C/Cdc2 pathway.

In addition to G2/M phase arrest, the levels of Histone H3 phosphorylation (Ser10), a well-established marker of mitosis, were determined to quantify the cells in the mitotic phase of the cell cycle. Phosphorylation at Ser10 of Histone H3 is tightly associated with chromosome condensation during mitosis (28), and it can act as part of a molecular mechanism driving mitotic chromosomal condensation during M phase entry (38). In this study, we found that irinotecan in combination with radiation resulted in a decreased and then increased M phase arrest. This indicated that the arrested cells were mostly present in the G2 phase at tge early time points after treatment, and arrested cells in M phase increased in the following 24 h. The cells probably underwent G2 phase arrest for a short period time and both G2 and M phase arrest occurred later. The cells arrested in the G2 or M phase probably died through mitotic catastrophe and apoptosis. The gradually enhanced apoptosis after cycle arrest in both cell lines was also confirmed in our experiments.

The present study has several limitations. First, we did not perform xenograft experiments to examine whether irinotecan exerts radiosensitizing effects on animals, which represents a condition more similar to the clinical setting. Second, experiments related to gene regulation were not performed in this study, including the upregulation and knockout of specific genes (such as Cdc25C and Wee1), which can aid in the verification of relevant molecular pathways. Third, experiments related to the mechanisms of apoptosis were not performed. The associations between the p53 status, cell cycle arrest and apoptosis in terms of irinotecan-induced radiosensitization remain unknown. Previous studies using irinotecan as a single agent have demonstrated that the DNA damage induced by irinotecan triggers long-term cell cycle arrest in p53-wild-type colorectal cancer cells and transient arrest, which is followed by the apoptosis of p53-mutant cells (29,39). Additionally, in p53-wild-type cells, the DNA damage-induced expression of p53 suppresses the mitotic checkpoint kinase hMps1 (human ortholog of the yeast monopolar spindle 1 kinase), and the lack of this suppression in p53-mutant cells contributes to apoptosis (40). In this study, we examined irinotecan as a radiosensitizer to and found that it induced marked G2/M phase arrest, followed by the enhanced apoptosis of p53-mutant colorectal cancer cells. However, whether this drug leads to the long-term cell cycle arrest of p53-wild-type colorectal cancer cells remains unclear. Thus, further studies are warranted to explore the above-mentioned mechanisms and to verify the results in animals.

The present study indicated that irinotecan could be used as an effective radiosensitizer in the pre-operative CRT of LARCs and may increase tumor regression rates, local control and, potentially, overall survival. To date, a number of phase I-II clinical trials have achieved pathologically complete response rates ranging from 13.7 to 37% (41-44), with a weekly irinotecan dose of 50-60 mg/m^2 in combination with fluoropyrimidine. Irinotecan should be used with caution in clinical treatments as of its adverse effects, such as diarrhea and neutropenia occur, particularly in UGT1A1/28 $^{*}1^{*}28$ and $^{*}28$ $^{*}28$ genotypes (45-47). Recently, Zhu *et al* (48) reported that the maximum tolerated doses (MTDs) of weekly irinotecan in neoadjuvant CRT for LARC were 80 mg/m^2 in patients with the $^{*}1^{*}1$ genotype and 65 mg/m^2 in those with the $^{*}1^{*}28$ genotype. A randomized, controlled phase III trial is currnelty ongoing to examine whether high-dose irinotecan can improve the clinical benefit under the guidance of the UGT1A1$^{*}28$ genotype in neoadjuvant therapy compared with standard capecitabine-based CRT (CinClare, NCT02605265).

In conclusion, this study demonstrates that irinotecan exerts radiosensitizing effects on HT29 and SW620 cells, and the SER increases with the increasing drug concentration. This effect is attributed to the activation of the DNA damage response system, leading to significant G2/M phase arrest,

followed by enhanced apoptosis, and this process likely occurs through the ATM/Chk/Cdc25C/Cdc2 pathway in p53-mutant colorectal cancer cells. Large-scale clinical trials are required to investigate not only the efficacy of irinotecan, but also its effects as a radiosensitizer.

Acknowledgements

The authors would like to thank American Journal Experts (https://www.aje.com) for assisting with language editing.

Funding

This study was supported by grants from the National Natural Science Foundation of China (no. 81572955).

Availability of data and materials

The datasets used and/or analyzed during the current study are available from the corresponding author on reasonable request.

Authors' contributions

YW, LY and JZ have full access to all of the findings in the study and take responsibility for the integrity of the data and the accuracy of the data analysis. ZZ, LL, MZ and YY provided the study concept and design. YW, LY, JZ and MZ were major contributors in performing the experiments. YW, LS, HZ, WY, RH and WD analyzed and interpreted the data. YW wrote the manuscript. MZ, RH, WY and YY reviewed and edited the manuscript. All authors have read and approved the final manuscript.

Ethics approval and consent to participate

Not applicable.

Patient consent for publication

Not applicable.

Competing interests

The authors declare that they have no competing interests.

References

1. Siegel RL, Miller KD and Jemal A: Cancer Statistics, 2017. CA Cancer J Clin 67: 7-30, 2017.
2. Sauer R, Becker H, Hohenberger W, Rödel C, Wittekind C, Fietkau R, Martus P, Tschmelitsch J, Hager E, Hess CF, *et al*; German Rectal Cancer Study Group: Preoperative versus postoperative chemoradiotherapy for rectal cancer. N Engl J Med 351: 1731-1740, 2004.
3. Bosset JF, Calais G, Mineur L, Maingon P, Radosevic-JelicL, Daban A, Bardet E, Beny A, Briffaux A and Collette L: Enhanced tumorocidal effect of chemotherapy with preoperative radiotherapy for rectal cancer: Preliminary results - EORTC 22921. J Clin Oncol 23: 5620-5627, 2005.
4. Bosset JF, Collette L, Calais G, Mineur L, Maingon P, Radosevic-Jelic L, Daban A, Bardet E, Beny A and Ollier JC; EORTC Radiotherapy Group Trial 22921: Chemotherapy with preoperative radiotherapy in rectal cancer. N Engl J Med 355: 1114-1123, 2006.
5. Ma B, Gao P, Wang H, Xu Q, Song Y, Huang X, Sun J, Zhao J, Luo J, Sun Y, *et al*: What has preoperative radio(chemo) therapy brought to localized rectal cancer patients in terms of perioperative and long-term outcomes over the past decades? A systematic review and meta-analysis based on 41,121 patients. Int J Cancer 141: 1052-1065, 2017.
6. Greenhalgh TA, Dearman C and Sharma RA: Combination of novel agents with radiotherapy to treat rectal cancer. Clin Oncol (R Coll Radiol) 28: 116-139, 2016.
7. Aschele C, Cionini L, Lonardi S, Pinto C, Cordio S, Rosati G, Artale S, Tagliagambe A, Ambrosini G, Rosetti P, *et al*: Primary tumor response to preoperative chemoradiation with or without oxaliplatin in locally advanced rectal cancer: Pathologic results of the STAR-01 randomized phase III trial. J Clin Oncol 29: 2773-2780, 2011.
8. Gérard JP, Azria D, Gourgou-Bourgade S, Martel-Laffay I, Hennequin C, Etienne PL, Vendrely V, François E, de La Roche G, Bouché O, *et al*: Comparison of two neoadjuvant chemoradiotherapy regimens for locally advanced rectal cancer: Results of the phase III trial ACCORD 12/0405-Prodige 2. J Clin Oncol 28: 1638-1644, 2010.
9. Rödel C, Liersch T, Becker H, Fietkau R, Hohenberger W, Hothorn T, Graeven U, Arnold D, Lang-Welzenbach M, Raab HR, *et al*; German Rectal Cancer Study Group: Preoperative chemoradiotherapy and postoperative chemotherapy with fluorouracil and oxaliplatin versus fluorouracil alone in locally advanced rectal cancer: Initial results of the German CAO/ARO/AIO-04 randomised phase 3 trial. Lancet Oncol 13: 679-687, 2012.
10. Allegra CJ, Yothers G, O'Connell MJ, Beart RW, Wozniak TF, Pitot HC, Shields AF, Landry JC, Ryan DP, Arora A, *et al*: Neoadjuvant 5-FU or capecitabine plus radiation with or without oxaliplatin in rectal cancer patients: A phase III randomized clinical trial. J Natl Cancer Inst 107: 107, 2015.
11. Fujita K, Kubota Y, Ishida H and Sasaki Y: Irinotecan, a key chemotherapeutic drug for metastatic colorectal cancer. World J Gastroenterol 21: 12234-12248, 2015.
12. Chabot GG: Clinical pharmacokinetics of irinotecan. Clin Pharmacokinet 33: 245-259, 1997.
13. Chen AY, Choy H and Rothenberg ML: DNA topoisomerase I-targeting drugs as radiation sensitizers. Oncology (Williston Park) 13 (Suppl 5): 39-46, 1999.
14. Mattern MR, Hofmann GA, McCabe FL and Johnson RK: Synergistic cell killing by ionizing radiation and topoisomerase I inhibitor topotecan (SK&F 104864). Cancer Res 51: 5813-5816, 1991.
15. Kim JH, Kim SH, Kolozsvary A and Khil MS: Potentiation of radiation response in human carcinoma cells in vitro and murine fibrosarcoma in vivo by topotecan, an inhibitor of DNA topoisomerase I. Int J Radiat Oncol Biol Phys 22: 515-518, 1992.
16. Boothman DA, Wang M, Schea RA, Burrows HL, Strickfaden S and Owens JK: Posttreatment exposure to camptothecin enhances the lethal effects of x-rays on radioresistant human malignant melanoma cells. Int J Radiat Oncol Biol Phys 24: 939-948, 1992.
17. Hennequin C, Giocanti N, Balosso J and Favaudon V: Interaction of ionizing radiation with the topoisomerase I poison camptothecin in growing V-79 and HeLa cells. Cancer Res 54: 1720-1728, 1994.
18. Chen AY, Scruggs PB, Geng L, Rothenberg ML and Hallahan DE: p53 and p21 are major cellular determinants for DNA topoisomerase I-mediated radiation sensitization in mammalian cells. Ann N Y Acad Sci 922: 298-300, 2000.
19. Yin L, Wu J, Wu J, Ye J, Jiang X, Chen M, Wang D, Wang X, Zong D, Gu J, *et al*: Radiosensitization effect of nedaplatin on nasopharyngeal carcinoma cells in different status of Epstein-Barr virus infection. BioMed Res Int 2014: 713674, 2014.
20. Jones L, Hoban P and Metcalfe P: The use of the linear quadratic model in radiotherapy: A review. Australas Phys Eng Sci Med 24: 132-146, 2001.
21. NCCN Clinical Practice Guidelines in Oncology Rectal Cancer Version 2.2018. J Natl Compr Canc Netw 16: 874-901, 2018..
22. Haug K, Kravik KL and De Angelis PM: Cellular response to irinotecan in colon cancer cell lines showing differential response to 5-fluorouracil. Anticancer Res 28A: 583-592, 2008.
23. Kaku Y, Tsuchiya A, Kanno T and Nishizaki T: Irinotecan induces cell cycle arrest, but not apoptosis or necrosis, in Caco-2 and CW2 colorectal cancer cell lines. Pharmacology 95: 154-159, 2015.
24. Pawlik TM and Keyomarsi K: Role of cell cycle in mediating sensitivity to radiotherapy. Int J Radiat Oncol Biol Phys 59: 928-942, 2004.

25. Stark GR and Taylor WR: Control of the G2/M transition. Mol Biotechnol 32: 227-248, 2006.
26. Taylor WR and Stark GR: Regulation of the G2/M transition by p53. Oncogene 20: 1803-1815, 2001.
27. Reinhardt HC and Yaffe MB: Kinases that control the cell cycle in response to DNA damage: Chk1, Chk2, and MK2. Curr Opin Cell Biol 21: 245-255, 2009.
28. Preuss U, Landsberg G and Scheidtmann KH: Novel mitosis-specific phosphorylation of histone H3 at Thr11 mediated by Dlk/ZIP kinase. Nucleic Acids Res 31: 878-885, 2003.
29. Bhonde MR, Hanski ML, Notter M, Gillissen BF, Daniel PT, Zeitz M and Hanski C: Equivalent effect of DNA damage-induced apoptotic cell death or long-term cell cycle arrest on colon carcinoma cell proliferation and tumour growth. Oncogene 25: 165-175, 2006.
30. Das P, Skibber JM, Rodriguez-Bigas MA, Feig BW, Chang GJ, Wolff RA, Eng C, Krishnan S, Janjan NA and Crane CH: Predictors of tumor response and downstaging in patients who receive preoperative chemoradiation for rectal cancer. Cancer 109: 1750-1755, 2007.
31. Chen AY, Chou R, Shih SJ, Lau D and Gandara D: Enhancement of radiotherapy with DNA topoisomerase I-targeted drugs. Crit Rev Oncol Hematol 50: 111-119, 2004.
32. Li TK and Liu LF: Tumor cell death induced by topoisomerase-targeting drugs. Annu Rev Pharmacol Toxicol 41: 53-77, 2001.
33. Chen AY, Okunieff P, Pommier Y and Mitchell JB: Mammalian DNA topoisomerase I mediates the enhancement of radiation cytotoxicity by camptothecin derivatives. Cancer Res 57: 1529-1536, 1997.
34. Omura M, Torigoe S and Kubota N: SN-38, a metabolite of the camptothecin derivative CPT-11, potentiates the cytotoxic effect of radiation in human colon adenocarcinoma cells grown as spheroids. Radiother Oncol 43: 197-201, 1997.
35. Jo HJ, Song JD, Kim KM, Cho YH, Kim KH and Park YC: Diallyl disulfide induces reversible G2/M phase arrest on a p53-independent mechanism in human colon cancer HCT-116 cells. Oncol Rep 19: 275-280, 2008.
36. Sur S and Agrawal DK: Phosphatases and kinases regulating CDC25 activity in the cell cycle: Clinical implications of CDC25 overexpression and potential treatment strategies. Mol Cell Biochem 416: 33-46, 2016.
37. Bartek J and Lukas J: Chk1 and Chk2 kinases in checkpoint control and cancer. Cancer Cell 3: 421-429, 2003.
38. Hendzel MJ, Wei Y, Mancini MA, Van Hooser A, Ranalli T, Brinkley BR, Bazett-Jones DP and Allis CD: Mitosis-specific phosphorylation of histone H3 initiates primarily within pericentromeric heterochromatin during G2 and spreads in an ordered fashion coincident with mitotic chromosome condensation. Chromosoma 106: 348-360, 1997.
39. Magrini R, Bhonde MR, Hanski ML, Notter M, Scherübl H, Boland CR, Zeitz M and Hanski C: Cellular effects of CPT-11 on colon carcinoma cells: Dependence on p53 and hMLH1 status. Int J Cancer 101: 23-31, 2002.
40. Bhonde MR, Hanski ML, Budczies J, Cao M, Gillissen B, Moorthy D, Simonetta F, Scherübl H, Truss M, Hagemeier C, *et al*: DNA damage-induced expression of p53 suppresses mitotic checkpoint kinase hMps1: The lack of this suppression in p53MUT cells contributes to apoptosis. J Biol Chem 281: 8675-8685, 2006.
41. Mohiuddin M, Winter K, Mitchell E, Hanna N, Yuen A, Nichols C, Shane R, Hayostek C and Willett C; Radiation Therapy Oncology Group Trial 0012: Randomized phase II study of neoadjuvant combined-modality chemoradiation for distal rectal cancer: Radiation Therapy Oncology Group Trial 0012. J Clin Oncol 24: 650-655, 2006.
42. Wong SJ, Moughan J, Meropol NJ, Anne PR, Kachnic LA, Rashid A, Watson JC, Mitchell EP, Pollock J, Lee RJ, *et al*: Efficacy endpoints of radiation therapy group protocol 0247: A randomized, phase 2 study of neoadjuvant radiation therapy plus concurrent capecitabine and irinotecan or capecitabine and oxaliplatin for patients with locally advanced rectal cancer. Int J Radiat Oncol Biol Phys 91: 116-123, 2015.
43. Mehta VK, Cho C, Ford JM, Jambalos C, Poen J, Koong A, Lin A, Bastidas JA, Young H, Dunphy EP, *et al*: Phase II trial of preoperative 3D conformal radiotherapy, protracted venous infusion 5-fluorouracil, and weekly CPT-11, followed by surgery for ultrasound-staged T3 rectal cancer. Int J Radiat Oncol Biol Phys 55: 132-137, 2003.
44. Navarro M, Dotor E, Rivera F, Sánchez-Rovira P, Vega-Villegas ME, Cervantes A, García JL, Gallén M and Aranda E: A Phase II study of preoperative radiotherapy and concomitant weekly irinotecan in combination with protracted venous infusion 5-fluorouracil, for resectable locally advanced rectal cancer. Int J Radiat Oncol Biol Phys 66: 201-205, 2006.
45. Liu X, Cheng D, Kuang Q, Liu G and Xu W: Association of UGT1A1*28 polymorphisms with irinotecan-induced toxicities in colorectal cancer: A meta-analysis in Caucasians. Pharmacogenomics J 14: 120-129, 2014.
46. Toffoli G, Cecchin E, Corona G, Russo A, Buonadonna A, D'Andrea M, Pasetto LM, Pessa S, Errante D, De Pangher V, *et al*: The role of UGT1A1*28 polymorphism in the pharmacodynamics and pharmacokinetics of irinotecan in patients with metastatic colorectal cancer. J Clin Oncol 24: 3061-3068, 2006.
47. Innocenti F, Undevia SD, Iyer L, Chen PX, Das S, Kocherginsky M, Karrison T, Janisch L, Ramírez J, Rudin CM, *et al*: Genetic variants in the UDP-glucuronosyltransferase 1A1 gene predict the risk of severe neutropenia of irinotecan. J Clin Oncol 22: 1382-1388, 2004.
48. Zhu J, Li X, Shen Y, Guan Y, Gu W, Lian P, Sheng W, Cai S and Zhang Z: Genotype-driven phase I study of weekly irinotecan in combination with capecitabine-based neoadjuvant chemoradiation for locally advanced rectal cancer. Radiother Oncol Radiother Oncol S0167-8140: 32749-32744, 2017.